Comparative Analysis of Reconfigurable Intelligent Surfaces and Relay Nodes for Energy Saving

Jordi Pérez-Romero[1], J. Xavier Salvat Lozano[2], Jose A. Ayala-Romero[2], Oriol Sallent[1], Anna Umbert[1], Juan Sánchez-González[1], Xavier Costa-Pérez[3,2]

[1]Universitat Politècnica de Catalunya (UPC), [2]NEC Laboratories Europe, [3]i2CAT Foundation and ICREA

***Abstract*—Different technologies are currently being investigated to reduce the energy consumption of beyond 5G systems. Two of the most preeminent ones are the Reconfigurable Intelligent Surfaces (RISs) and the relays, as both of them allow reducing the overall transmitted power levels at the base stations. However, due to the different nature of the two approaches, RISs being mostly passive while relays being active devices, it is unclear in which conditions one or the other leads to higher energy savings. This paper intends to shed light on this question by presenting a thorough analytical study of both approaches. Compared to the current literature, this study goes a step further by considering a more accurate RIS modeling based on actual RIS equipment, a thorough comparison of different energy consumption models, and a comprehensive study in a realistic environment of a university campus including indoor and outdoor propagation.**

Keywords—Reconfigurable intelligent surface (RIS); relay; energy saving; Beyond 5G

I. INTRODUCTION

Reconfigurable Intelligent Surfaces (RISs) have recently emerged as a key technology for next-generation mobile systems [1]. A RIS can reflect or absorb radio signals, altering the propagation environment. Also, a RIS can enable passive beamforming gains by focusing radio signals towards a receiver without relying on energy-intensive power amplifiers or baseband processors. Thus, RISs are well-perceived as an energy-efficient and inexpensive enabler in many 6G use cases [2][3]. They also contribute to reducing the required transmit power at the base stations and thus the overall energy consumption in the network. However, it is not clear what are the gains of RIS with respect to other traditional active devices such as relays, which are also able to reduce the transmitted power requirements leading also to energy savings [4]. Relays, in contrast to RIS, are active devices and are enabled with power amplifiers and baseband processors. For this reason, they can also amplify the signal but at the cost of higher energy consumption and higher OPEX.

In this paper, we conduct a thorough analytical comparison between RISs and relays, attending to their particularities in terms of how they alter the radio propagation environment and their energy savings. We study the different trade-offs and practical benefits as a function of different factors such as location deployment, RIS' codebook configuration, path loss values or power consumption model parameters.

Some previous works compare RISs with traditional relays. Some of them focus on RIS vs. amplify-and-forward (AF) relays, with AF relays generally outperforming RIS in spectral efficiency but RIS offering better energy efficiency [5]. Large RISs can potentially surpass AF relays in signal-to-noise ratio (SNR) [6]. RIS has also been compared to decode-and-forward (DF) relays, with RIS achieving higher energy efficiency at high data rates, though requiring many elements [7][8]. In comparison with full-duplex relays, a RIS generally lags in data rate unless it has many elements, but it outperforms DF relays in energy efficiency [9][10][11]. Finally, a study in London [2] explores deploying RISs in urban areas with poor coverage, finding it to be a cost-efficient alternative to traditional network expansions, though not matching conventional technologies in coverage and data rate.

In contrast to these previous works, our study goes a step further by considering different aspects not addressed in the literature. First, we consider a more accurate RIS modelling based on physical constraints of actual RIS equipment. In particular, we consider a codebook characterized using a RIS prototype [12]. Second, we analyze the impact of aspects that are underexplored in the literature, such as the values of the power consumption model parameters of the considered equipment, the impact of the radiation pattern in different directions in accordance with the measurement-based RIS model or the impact of the propagation losses between the base station and the RIS/relay. Finally, the paper also presents a comparison of RISs and relays in a realistic scenario that represents the university campus of UPC in Barcelona. It includes different buildings and combines indoor and outdoor propagation effects to assess the best approach for different conditions and under realistic locations.

The paper is organized as follows. Section II presents the model of the cellular network with relays and RISs and the considered key performance indicators (KPIs). Then, Section III presents a first comparison between both approaches analyzing the impact of different model parameters. This analysis is further extended in Section IV through simulations in a realistic scenario representing a university campus area. Finally, conclusions are summarized in Section V.

II. SYSTEM MODEL

Let us assume the downlink communication between a base station (BS) and a User Equipment (UE) that requires a bit rate R_{UE}. The possibility of deploying a relay node or a RIS at a given position is considered. This is illustrated in Fig. 1, which shows the different communication options that are modelled in the following subsections.

This work has been partially funded by the Smart Networks and Services Joint Undertaking (SNS JU) under the European Union's Horizon Europe research and innovation program under Grant Agreement No. 101097083 (BeGREEN project) and by grants ARTIST (PID2020-115104RB-I00) and TRAINER-6G (PID2023-146748OB-I00) funded by MCIN/AEI/10.13039/501100011033 and by ERDF/EU. Views and opinions expressed are however those of the authors only and do not necessarily reflect those of the European Union or the other granting authorities. Neither the European Union nor the granting authority can be held responsible for them.

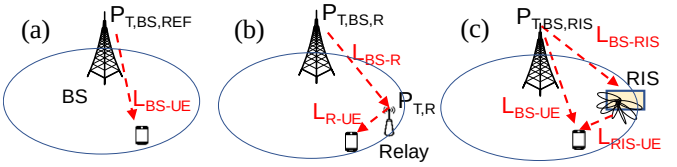

Fig. 1. Considered communication options. (a) Reference case. (b) Use of a relay node. (c) Use of a RIS.

A. *Reference case model*

Fig. 1a considers the reference case in which the UE is directly connected to the BS without the support of any relay or RIS. The total propagation loss between the BS and the UE is $L_{BS\text{-}UE}$ and the required transmitted power at the BS to support the bit rate is denoted as $P_{T,BS,REF}$. The relationship between the transmitted power and the bit rate of the UE is obtained from the Shannon formula as:

$$P_{T,BS,REF} = \left(2^{\frac{R_{UE}}{B_{BS} \cdot \varepsilon_{BS}}} - 1 \right) \frac{P_{N,UE} L_{BS-UE}}{G_{BS} G_{UE}} \quad (1)$$

where G_{BS}, G_{UE} are the gains of the antennas of the BS and the UE, B_{BS} is the transmission bandwidth, $P_{N,UE}$ is the noise power at the UE measured over this bandwidth and ε_{BS} is an efficiency factor $0 < \varepsilon_{BS} \leq 1$ that accounts for the overheads associated to cyclic prefix, reference signals, control plane signaling, etc.

Then, following the model of references such as [13][14] the total power consumption at the BS is given by:

$$P_{TOT,REF} = a_{BS} P_{T,BS,REF} + P_{0,BS} \quad (2)$$

where a_{BS} is a scaling factor that determines the contribution of the transmitted power and $P_{0,BS}$ is the consumption at zero RF output power due to circuits, signal processing, etc.

B. *Relay model*

Fig. 1b depicts the situation where a relay node is deployed at a certain position. The UE is served by the relay node and connects to the BS in two hops, namely the Relay-UE link with propagation loss $L_{R\text{-}UE}$ and the BS-Relay link with propagation loss $L_{BS\text{-}R}$. A DF relay is considered with out-of-band operation, i.e. the Relay-UE and BS-Relay links operate at different frequencies. In this way, the relay operation does not affect the available bandwidth at the BS, as it would occur with an in-band relay. The transmitted power by the BS in this case, denoted as $P_{T,BS,R}$, is determined by the power required to provide the bit rate R_{UE} in the BS-Relay link, that is:

$$P_{T,BS,R} = \left(2^{\frac{R_{UE}}{B_{BS} \cdot \varepsilon_{BS}}} - 1 \right) \frac{P_{N,R} L_{BS-R}}{G_{BS} G_{R}} \quad (3)$$

where G_R is the antenna gain of the relay and $P_{N,R}$ the noise power of the relay receiver in the BS-Relay link.

Similarly, the required transmitted power of the relay node to provide the bit rate R_{UE} in the Relay-UE link is:

$$P_{T,R} = \left(2^{\frac{R_{UE}}{B_{R} \cdot \varepsilon_{R}}} - 1 \right) \frac{P_{N,UE,R} L_{R-UE}}{G_{R} G_{UE}} \quad (4)$$

where B_R is the transmission bandwidth in the Relay-UE link, $P_{N,UE,R}$ is the noise power at the UE measured over this bandwidth and ε_R is the efficiency factor that accounts for the overheads.

The total power consumption is the aggregate of the power consumed by the BS and the relay, given by:

$$P_{TOT,REL} = a_{BS} P_{T,BS,R} + P_{0,BS} + a_{R} P_{T,R} + P_{0,R} \quad (5)$$

where a_R and $P_{0,R}$ are, respectively, the scaling factor of the transmitted power and the power consumption at zero RF power for the relay.

C. *RIS model*

RISs are structures designed to alter the reflection behavior of impinging radio waves without requiring complex RF chains. A RIS board is usually arranged as a planar antenna array with $N=N_i \times N_j$ unit cells (e.g. patch antennas) separated by a fixed sub wavelength distance. Fig. 1c depicts a situation in which a RIS reflects a signal towards a UE. $L_{BS\text{-}RIS}$ and $L_{RIS\text{-}UE}$ denote, respectively, the propagation losses in the links BS-RIS and RIS-UE. The ability of the RIS to reflect the received signal from a BS in the direction of the UE depends on the phase shifts applied by its elements. Fig. 2 depicts the reference system of the RIS based on a horizontal coordinate system. We denote the azimuth angles between the BS-RIS and RIS-UE as θ_t and θ_r, respectively. They are defined with respect to right hand side part of a RIS board in the range of [-180°,0°]. Similarly, we denote ϕ_t and ϕ_r, respectively, as the elevation with respect to the perpendicular of the RIS in the range [-90°,+90°]. In practice, the range of operation of an RIS is limited to [-150°, -30°] in the azimuth and [-45°,+45°] in the elevation range [12].

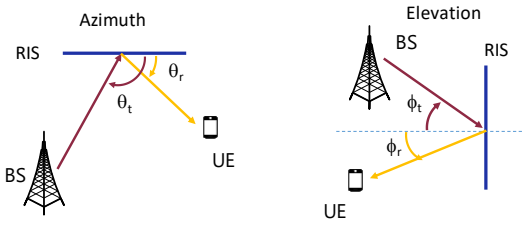

Fig. 2. Angles in azimuth and elevation for the BS-RIS and RIS-UE links.

The received power $P_{R,UE}$ at the UE when reflecting a signal using the RIS results from aggregating the direct path between BS and UE and the reflected path at the RIS. It is given by:

$$P_{R,UE} = \frac{P_{T,BS,RIS} G_{BS} G_{UE}}{L_{RIS}} \quad (6)$$

$$L_{RIS} = \frac{1}{\left\| \frac{D(\theta_r, \phi_r)^{*} \cdot \Theta \cdot D(\theta_t, \phi_t)}{\sqrt{L_{BS-RIS} L_{RIS-UE}}} + \frac{1}{\sqrt{L_{BS-UE}}} \right\|^2} \quad (7)$$

where $D(\theta_t,\phi_t)$ and $D(\theta_r,\phi_r)$ are $\mathbb{C}^{1\times N}$ vectors corresponding to the array response of the RIS in the directions BS-RIS and RIS-UE, respectively. Θ is a diagonal $N \times N$ matrix defined as:

$$\Theta = diag\left[e^{j\theta_1}, ..., e^{j\theta_N} \right] \quad (8)$$

where the values θ_n $n \in \{1,...,N\}$ are the phase shifts configured

for each one of the N RIS elements. The element in the cell of row i and column j is mapped to index $n=n_i+(n_j-1)\cdot N_i$ $\forall n_i \in \{1,...,N_i\}$, $n_j \in \{1,...,N_j\}$. Θ is selected from a codebook to maximize the reflected power from the direction of the impinging signal towards the desired direction.

Then, the transmitted power required by the BS in order to provide the required bit rate R_{UE} is given by:

$$P_{T,BS,RIS} = \left(2^{\frac{R_{UE}}{B_{BS} \cdot \varepsilon_{BS}}} - 1 \right) \frac{P_{N,UE} L_{RIS}}{G_{BS} G_{UE}} \quad (9)$$

The total power consumption is the aggregate of the power consumed by the BS and the power consumed by the RIS, denoted as P_{RIS}. This yields:

$$P_{TOT,RIS} = a_{BS} P_{T,BS,RIS} + P_{0,BS} + P_{RIS} \quad (10)$$

D. Key Performance Indicators

To conduct the comparison between RISs and relays, a set of KPIs is considered. Firstly, the energy or power saving with respect to the reference case is defined for the relay and the RIS, respectively, as:

$$ES_{REL}(\%) = 100 \left(\frac{P_{TOT,REF} - P_{TOT,REL}}{P_{TOT,REF}} \right) \quad (11)$$

$$ES_{RIS}(\%) = 100 \left(\frac{P_{TOT,REF} - P_{TOT,RIS}}{P_{TOT,REF}} \right) \quad (12)$$

In turn, the power consumption reduction (PCR) of the relay with respect to the RIS is defined as:

$$PCR(\%) = 100 \left(\frac{P_{TOT,RIS} - P_{TOT,REL}}{P_{TOT,RIS}} \right) \quad (13)$$

Note that PCR>0% means that the relay requires less power than the RIS, while PCR<0% means that the RIS requires less power than the relay.

III. Impact of Model Parameters

This section assesses how the different model parameters of the considered scenario with RIS or relays impact on the achieved energy savings. The three cases illustrated in Fig. 1 are considered, assuming that the relay and the RIS are placed at the same location, so that $L_{BS\text{-}RIS}$=$L_{BS\text{-}R}$ and $L_{RIS\text{-}UE}$=$L_{R\text{-}UE}$. The values of the parameters in the evaluation are presented in Table I, indicating those that are varied. The RIS codebook for reflecting a signal to a specific direction has been computed analytically and validated from measurements on actual RIS equipment [12]. The RIS power consumption value is also based on this equipment. To assess the impact of the azimuth angle between the UE and the RIS, it is assumed that the RIS codebook is optimized to reflect the BS power in the direction of a receiver at azimuth -120° and elevation -20°, while the actual azimuth θ_r of the UE is varied to capture the performance of the RIS in different directions. In turn, different values of the propagation loss $L_{BS\text{-}RIS}$ between the BS and the RIS or relay are considered, representing different distances between them. Regarding the parameters of the power consumption model for the BS and the relay, eight possible combinations C1,..., C8 are tested, based on different values extracted from references [4][13][15].

TABLE I. Model Parameters

Parameter	Value	
Ant. gains	G_{BS} = 10 dB, G_R = 3 dB, G_{UE} = 3 dB	
Bandwidth	B_{BS} = [20, 100] MHz, B_R = 20 MHz	
Noise power	$P_{N,UE} = P_{N,R} = N_o B_{BS}$, $P_{N,R,UE} = N_o B_R$ with N_o=-168 dBm/Hz	
Eff. factor	$\varepsilon_{BS} = \varepsilon_R$ = 0.59	
Bit rate	50 Mb/s	
Angles	BS-RIS: θ_t=-90°, ϕ_t=5°, RIS-UE: θ_r varied, ϕ_t=-20°	
Prop. losses	$L_{BS\text{-}RIS} = L_{BS\text{-}R}$ varied, $L_{RIS\text{-}UE} = L_{R\text{-}UE}$=70 dB, $L_{BS\text{-}UE}$=140 dB	
RIS	10×10 elements, Codebook optimized for a receiver at azimuth -120°, elevation -20°, P_{RIS}=62 mW	
Power consumption parameters of BS and relay	C1	a_{BS}=28.4, $P_{0,BS}$=156.38 W, a_R=20.4, $P_{0,R}$=13.91 W
	C2	a_{BS}=28.4, $P_{0,BS}$=156.38 W, a_R=4, $P_{0,R}$=6.8 W
	C3	a_{BS}=4.7, $P_{0,BS}$=130 W, a_R=20.4, $P_{0,R}$=13.91 W
	C4	a_{BS}=4.7, $P_{0,BS}$=130 W, a_R=4, $P_{0,R}$=6.8 W
	C5	a_{BS}=2.8, $P_{0,BS}$=84 W, a_R=20.4, $P_{0,R}$=13.91 W
	C6	a_{BS}=2.8, $P_{0,BS}$=84 W, a_R=4, $P_{0,R}$=6.8 W
	C7	a_{BS}=2.57, $P_{0,BS}$=12.85 W, a_R=20.4, $P_{0,R}$=13.91 W
	C8	a_{BS}=2.57, $P_{0,BS}$=12.85 W, a_R=4, $P_{0,R}$=6.8 W

Fig. 3a shows the energy saving values achieved with the relay and the RIS with respect to the reference case as a function of the azimuth angle θ_r of the UE for the case $L_{BS\text{-}RIS}$ = 70 dB. This path loss could correspond e.g. to a distance of 30m with an UMi model in Line of Sight (LOS), so that the RIS or relay are located close to the BS. In turn, Fig. 3b shows the case $L_{BS\text{-}RIS}$ = 100 dB, which could correspond e.g. to a distance of 500m with an UMa model in LOS. Results consider bandwidth B_{BS}=20 MHz and combination C1 of power consumption parameters. It is observed that the energy saving achieved with the relay is very similar in both cases. In turn, when using the RIS, the energy savings reduce significantly when the path loss between the BS and the RIS increases. Besides that, with the RIS, the energy savings fluctuate a lot depending on the azimuth angle, capturing the radiation pattern of the RIS. This is particularly noticeable for $L_{BS\text{-}RIS}$ = 100 dB, in which the maximum energy saving is only achieved in a range of approximately +/- 5° around the direction of -120° that corresponds to the maximum reflected power according to the codebook configuration (denoted as "Codebook UE" in the figures). In the rest of directions, the energy savings reduce in more than one half and are much lower than those of the relay.

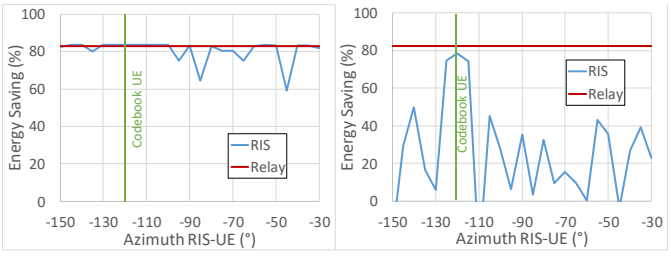

Fig. 3. Energy saving achieved for different θ_r values with (a) $L_{BS\text{-}RIS}$=70 dB, (b) $L_{BS\text{-}RIS}$=100 dB

The comparison between the relay and the RIS in terms of the PCR metric is shown in Fig. 4 considering the two values $L_{BS\text{-}RIS}$=70 dB and $L_{BS\text{-}RIS}$=100 dB as well as two different BS bandwidths, namely B_{BS}=20 MHz and B_{BS}=100 MHz. When the RIS or relay are close to the BS, corresponding to the low path loss value of 70 dB, there are several angles in which the RIS achieves lower power consumption than the relay, i.e. PCR<0%, mostly in a span of +/- 30° around the angle of -120° where the RIS reflects the highest power. For these angles, the power consumption with the relay is up to about 9% higher than with the RIS. Outside these angles, the RIS performance degrades with a lot of fluctuations depending on the angle, and the relay starts to go better, i.e. PCR>0% with values up to 56% for bandwidth 20 MHz and 18% for bandwidth 100 MHz.

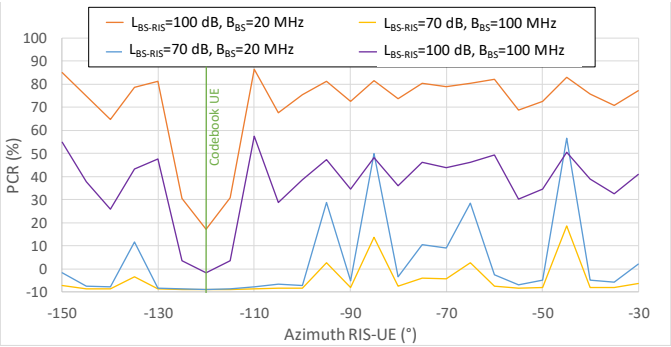

Fig. 4. PCR metric as a function of the azimuth θ_r.

When the RIS/relay is farther from the BS, i.e. path loss of 100 dB in Fig. 4, the effect of the RIS is only noticeable in an angle of about +/- 5° around the angle of -120°. Still, in this region the RIS performs very similar to the relay (PCR ~ 0%) for B_{BS}=100 MHz and worse than the relay (PCR ~ 17%) for B_{BS} =20 MHz. For the rest of angles, the PCR varies between 65% and 85% for 20 MHz and between 30% and 60% for 100 MHz.

To further assess the impact of the propagation losses, or equivalently distance, between the BS and the relay/RIS, Fig. 5 plots the energy saving with respect to the reference case achieved by the RIS and by the relay as a function of $L_{BS\text{-}RIS}$ when the UE is located at the optimum angle of -120° according to the RIS codebook configuration. B_{BS}=20 MHz and combination C1 of power consumption parameters are considered. It is observed that the RIS provides a bit higher savings than the relay when $L_{BS\text{-}RIS}$<90 dB, and these are kept more or less constant. Instead, the relay provides higher savings for 90 dB<$L_{BS\text{-}RIS}$<140 dB. For $L_{BS\text{-}RIS}$ above 140 dB, both techniques bring very little or no energy savings with respect to the reference case.

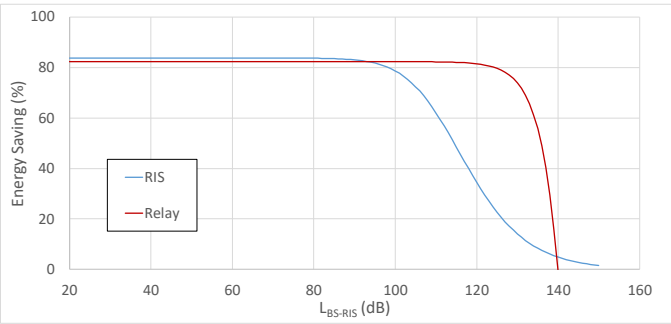

Fig. 5. Energy saving as a function of the path loss between BS and RIS/relay.

The effect of the power consumption model parameters of the BS and relay is shown in Fig. 6. It plots the PCR metric as a function of the path loss $L_{BS\text{-}RIS}$ for the different combinations of power consumption model parameters indicated in Table I. The figure considers the UE located at the optimum angle -120° based on the RIS codebook and bandwidth B_{BS}=20 MHz. It is observed that the improvements of the RIS with respect to the relay are very sensitive to the power consumption model parameters. For low path loss (i.e. up to $L_{BS\text{-}RIS}$=90 dB) the RIS outperforms the relay (i.e. PCR<0%). However, there are larger differences for the cases with lower $P_{0,BS}$, i.e. combination C7, which leads to a PCR of about -110%, and combination C8, which shows a PCR of about 50%. In the other combinations, PCR is about -10%. In turn, for $L_{BS\text{-}RIS}$>90 dB the relay starts to perform better and achieves PCR>0% for all combinations. The maximum values of the PCR are obtained for a path loss of approximately 125 dB and range from 25% for combination C5 up to 70% for combinations C1 and C2.

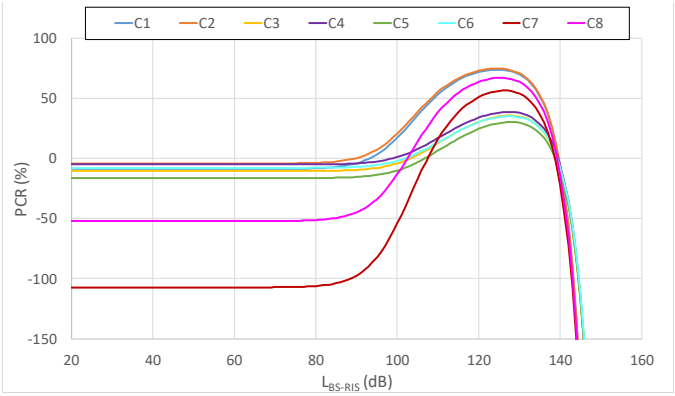

Fig. 6. Impact of the power consumption parameters on the PCR metric.

IV. Assessment in a Campus Scenario

This section presents the results of the comparison between the use of RISs and relays in a realistic scenario that comprises the university campus of UPC in Barcelona. The environment is a 350 m × 125 m area with 25 buildings of 3 floors as depicted in Fig. 7, where the modelled area corresponds to the rectangle highlighted in red. The names of the buildings A1,...,D6 are also included in the figure. 5G NR coverage on the campus is provided by three outdoor macrocells of a public operator in band n78 (3.3-3.8 GHz). The locations of the these macrocells are shown in the figure. The Urban Macrocell (UMa) propagation model of 3GPP TR 38.901 at 3.7 GHz is used for evaluating the propagation conditions at the different locations of the modelled area, subdivided in square pixels of 1 m × 1 m. The path loss includes 2D-spatially correlated shadowing and outdoor-to-indoor penetration loss for indoor positions.

An analysis of the path loss values in this scenario reflects that the poor coverage areas with high path loss values are located indoor. In this respect, Fig. 8 plots the path loss experienced at the different locations in the ground level with the base station BS2, which is the one that serves the largest area in the campus. As it can be observed, the outdoor path loss values are approximately below 110 dB in most of the cases, while the indoor path losses are larger than 130 dB in many positions. Then, a first study has consisted in analyzing 10 indoor positions with poor coverage at different floors of the

buildings that are closer to BS2 and analyzing two alternatives to enhance the coverage of each one, namely the use of an indoor or an outdoor RIS/relay. This leads to the 20 situations depicted in Fig. 8, each one represented by an arrow in which the tip is the UE position and the circle the RIS/relay position (indoor for situations 1 to 10 and outdoor for situations 11 to 20). The RIS codebook is always configured to reflect the maximum power in the direction of the UE. The propagation losses of the link RIS/relay-UE are obtained with the Indoor Hotspot (InH) model and the Urban Microcell (UMi) respectively for indoor and outdoor RIS/relays. The rest of parameters are those of Table I with B_{BS}=20 MHz and combination C1.

Fig. 7. University campus scenario.

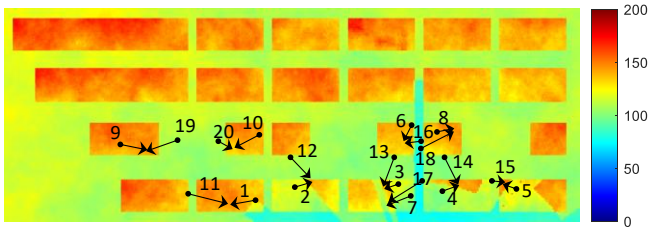

Fig. 8. Path loss values at ground level and studied situations. Locations are in the ground floor for cases 1, 2, 3, 5, 11, 12, 13, 15, in the 1st floor for cases 4, 6, 7, 10, 14, 16, 17, 20 and in the 2nd floor for cases 8, 9, 18, 19.

Fig. 9 depicts the PCR metric for each situation as a function of the path loss between the BS and the RIS/relay in Fig. 9a and of the path loss between the RIS/relay and the UE in Fig. 9b. In turn, the energy savings with respect to the reference case for the relay and the RIS are depicted in Fig. 10. It is observed that in all the situations with an indoor RIS/relay the relay outperforms the RIS, i.e. PCR>0% in Fig. 9 and ES_{REL}>ES_{RIS} in Fig. 10. The main reason is the large path loss between the BS and the RIS/relay that exists in these situations. Indeed, this corroborates the results in previous section (see Fig. 5) that indicate that the RIS needs to have a good path loss with the BS (e.g. lower than ~90 dB, which is hardly found in indoor locations) to achieve higher energy savings than the relay. In turn, looking at the situations 11 to 20 in which the RIS/relay is outdoor, it is observed in Fig. 9a that the path loss $L_{BS\text{-}RIS}$ is in general smaller than when it is indoor and, as result, in situations 14, 16, 17, 18 the RIS requires less power than the relay, i.e. PCR<0%. Among them, the situations 16, 17 and 18 are characterized by very low values of $L_{BS\text{-}RIS}$ < 85 dB, while the situation 14 has a larger value of $L_{BS\text{-}RIS}$ (~97 dB) but, in contrast, the path loss $L_{RIS\text{-}UE}$ is much lower than in the other situations (see Fig. 9b). In turn, the rest of outdoor situations with PCR>0% are characterized by lower values of $L_{BS\text{-}RIS}$ than for the indoor situations but by higher values of $L_{RIS\text{-}UE}$, leading eventually to a better performance of the relay. In terms of energy savings with respect to the reference case, it is seen in Fig. 10 that in all the situations the RIS and the relay achieve significant savings, being more than 90% in some of them. In most of the situations, the energy savings of the relay are larger than those of the RIS, while in the abovementioned four situations with PCR<0% the energy saving of the RIS is slightly higher than that of the relay.

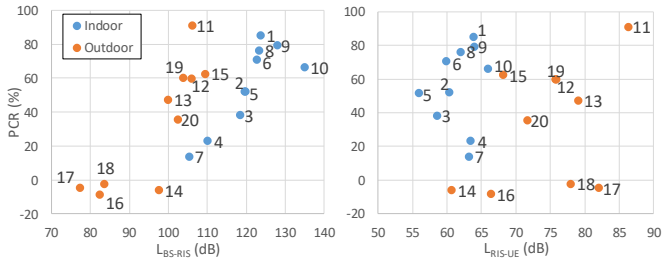

Fig. 9. PCR metric for the studied situations as a function of the path loss between BS and RIS/relay (a) and between RIS/relay and UE (b).

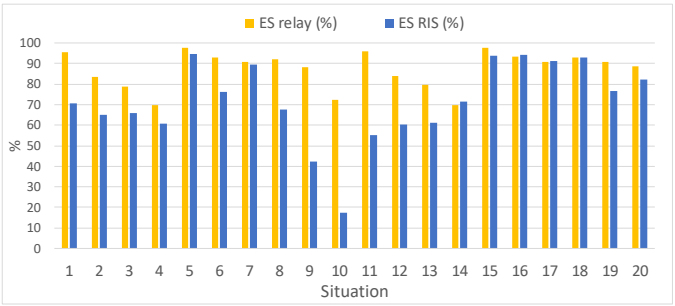

Fig. 10. Energy saving with the relay and the RIS for each studied situation.

To get further insights into one of the situations with PCR<0%, a more detailed analysis of the RIS/relay used in situation 14 is conducted. In this case, the RIS/relay is deployed close to the wall of building B5 to improve a coverage hole at the first floor of building A5. The RIS reflects the signal of BS2 and is initially configured with a codebook to point in the direction shown in Fig. 8 that corresponds to azimuth θ_r=-80°. Fig. 11 plots the map of the first floor of building A5 with the value of the PCR metric for each pixel. This has been obtained considering a UE located at each pixel and assessing the required power consumption when it is connected through the relay or through the RIS.

Fig. 11. PCR metric at the first floor of A5 building.

The pixels in which the RIS results in less power consumption than the relay (i.e. PCR<0%) correspond to the grey area at the central upper part of Fig. 11. This represents approximately 5% of the pixels in the floor. The lowest PCR

value achieved in these pixels is around -7.7% (i.e. the relay requires 7.7% more power than the RIS). These pixels belong to the coverage hole area and fall around the azimuth angle where the RIS reflects most of the power based on its codebook configuration. In contrast, the rest of pixels in yellow/green in the upper part of the building are those of the coverage hole in which the use of the relay leads to a lower power consumption than the RIS and represent approximately 21% of the pixels. In the rest of pixels of the floor where the BS coverage is sufficiently good there are no differences between relay and RIS (i.e. PCR ~0%) because, in this area, none of the two approaches leads to energy savings with respect to the reference case. This area is approximately 74% of the building.

To assess the effect of the pointing direction of the RIS based on its codebook configuration, Fig. 12 plots in blue the percentage of pixels of the ground floor of the building in which the RIS requires less power than the relay and there is energy saving with respect to the reference case. Similarly, it plots in orange the percentage of pixels in which the relay requires less power than the RIS and there is energy saving with respect to the reference case. These percentages are presented as a function of the RIS pointing direction. Fig. 12 shows that in all the cases the relay leads to lower consumption in a larger number of pixels than the RIS, with a percentage fluctuating between 21% and 25% depending on the direction. Instead, the percentage of pixels in which the RIS outperforms the relay varies between 0 and 6%, with the highest values for pointing directions between -100° and -70°. In these cases, the RIS reflects the power to a larger part of the coverage hole. In the rest of pixels of the floor not included in the percentages of Fig. 12 neither the RIS nor the relay achieve significant energy savings with respect to the reference case. These are approximately 76% of the pixels.

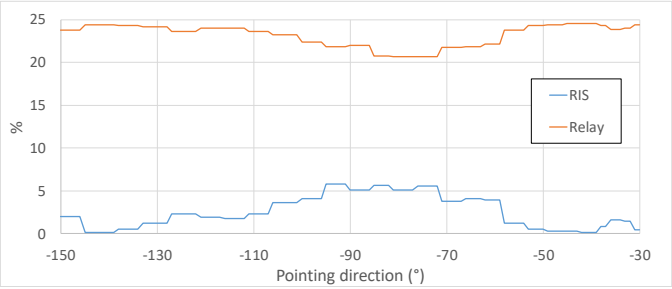

Fig. 12. Percentage of pixels of the ground floor where the RIS (or relay) requires less power than the relay (or RIS) as a function of the pointing angle.

V. Conclusions and Future Work

This paper has compared the use of a RIS or a relay in terms of achievable energy savings with respect to the case when none of these elements is used. Results have shown that both approaches can achieve substantial energy savings of up to 80%-90% in some cases with respect to this reference case.

The comparison between the two approaches depends on several factors. In general, the RIS achieves higher savings than the relay when the path loss between the RIS and the base station is low, e.g. up to ~70-90 dB, and the UE is in an angular region of up to +/- 30° with respect to the RIS pointing angle. In this case, the power consumption with the RIS is ~9% lower than with the relay. For larger path loss values or when the UE is outside these angular ranges, the relay outperforms the RIS. It has also been found that the comparison is very sensitive to the power consumption model parameters that characterize the consumption at zero RF power and the scale factor with the transmitted power. Depending on them, the RIS can outperform the relay with differences between 10% and 110% for low path loss values between RIS and BS, while for high path loss values the relay outperforms the RIS in about 25% to 70%.

The analysis in the UPC campus scenario has concluded that in most of the analyzed situations the relay provides higher energy savings than the RIS. The reason is that the areas with poor coverage in the campus are located indoor and an indoor RIS to cover these areas would experience an excessive path loss with the BS. Thus, the RIS can only provide better savings than the relay in very specific conditions of outdoor RIS. In these cases, the RIS improvements over the relay are observed mostly in a small area around the RIS pointing direction.

The presented results have considered an out-of-band relay in order not to affect the operation of the BS. However, this also means that deploying the relay requires additional bandwidth than deploying the RIS. In this regard, further comparisons for in-band relays can also be of interest and are left as future work.

References

[1] G. C. Trichopoulos, "Design and evaluation of reconfigurable intelligent surfaces in real-world environment," *IEEE Open Journal of the Communications Society*, Vol. 3, 2022.

[2] M. Rossanese, et al., "Data-driven analysis of the cost-performance trade-off of reconfigurable intelligent surfaces in a production network," *Proceedings of the ACM on Networking*, Vol. 1, CoNEXT3, 2023.

[3] P. Mursia, et al., "RISMA: Reconfigurable intelligent surfaces enabling beamforming for IoT massive access," *IEEE Journal on Selected Areas in Communications*, Vol. 39, No. 4, 2020.

[4] R. Fantini, D. Sabella, M. Caretti, "An E3F based assessment of energy efficiency of Relay Nodes in LTE-Advanced networks," *IEEE Symp. on Personal, Indoor and Mobile Radio Comm. (PIMRC)*, Toronto, 2011.

[5] C. Huang, A. Zappone, G. C. Alexandropoulos, M. Debbah, C. Yuen, "Reconfigurable intelligent surfaces for energy efficiency in wireless communication," *IEEE Trans. on Wir. Comm.*, Vol. 18, No. 8, 2019.

[6] A-A. A. Boulogeorgos, A. Alexiou, "Performance analysis of reconfigurable intelligent surface-assisted wireless systems and comparison with relaying," *IEEE Access*, Vol. 8, 2020.

[7] E. Björnson, Ö. Özdogan, E. G. Larsson, "Intelligent reflecting surface versus decode-and-forward: How large surfaces are needed to beat relaying?," *IEEE Wir. Comms. Letters*, Vol. 9, No. 2, 2020.

[8] I. Chatzigeorgiou, "The impact of 5G channel models on the performance of intelligent reflecting surfaces and decode-and-forward relaying," *IEEE Symp. on Personal, Indoor and Mobile Radio Comm. (PIMRC)*, London, 2020.

[9] A. Bazrafkan, et al., "Performance comparison between a simple full-duplex multi-antenna relay and a passive reflecting intelligent surface," *IEEE Trans. on Wir. Comms.*, Vol. 22, No. 8, 2023.

[10] M. Di Renzo, et al., "Reconfigurable intelligent surfaces vs. relaying: Differences, similarities, and performance comparison," *IEEE Open Journal of the Communications Society*, Vol. 1, 2020.

[11] J. Ye, et al., "Spatially-distributed RISs vs relay-assisted systems: A fair comparison," *IEEE Open Journal of the Communications Society*, 2021.

[12] M. Rossanese, et al., "Designing, building, and characterizing RF switch-based reconfigurable intelligent surfaces," *ACM Workshop on Wireless Network Testbeds, Experimental evaluation & CHaracterization*, 2022.

[13] G. Auer et al., "How much energy is needed to run a wireless network?," *IEEE Wir. Comms.*, Vol. 18, No. 5, Oct. 2011

[14] EARTH project, "D2.3 - Energy efficiency analysis of the reference systems, areas of improvements and target breakdown", Jan 2012.

[15] E. Björnson, et al., "Massive MIMO and small cells: Improving energy efficiency by optimal soft-cell coordination," *Int. Conf. Telecom. (ICT)*, Casablanca, 2013